Algal Research 52 (2020) 102094

Contents lists available at ScienceDirect

Algal Research

journal homepage: www.elsevier.com/locate/algal

Photosystems I and II in *Ulva lactuca* are well protected from high incident sunlight

Di Zhang[a], Sven Beer[c], He Li[a], Kunshan Gao[a,b,*]

[a] State Key Laboratory of Marine Environmental Science, College of Ocean and Earth Sciences, Xiamen University, Xiamen 361102, China
[b] Co-Innovation Center of Jiangsu Marine Bio-industry Technology, Jiangsu Ocean University, Lianyungang 222005, China
[c] Department of Plant Sciences and Food Security, Faculty of Life Sciences, Tel Aviv University, Tel Aviv 6997801, Israel

ARTICLE INFO

Keywords:
Chlorophyll fluorescence
Diurnal fluctuations
Photosynthetic light reactions
Photosystems II
Photosystem I
Ulva lactuca

ABSTRACT

We investigated the individual as well as combined performance of photosystem II and photosystem I in the ubiquitous green macroalga *Ulva lactuca* under diurnally changing light conditions using a dual pulse-amplitude modulated chlorophyll fluorescence technique. Along with rising levels of sunlight, the effective and maximal quantum yields of photosystem II decreased with increasing non-photochemical quenching. With declining irradiances in the afternoon, these photosystem II characteristics recovered gradually, such that they reached the same levels in the evening as in the morning without any signs of photodamage during the day. The values of non-photochemical quenching were higher in the afternoon than during pre-noon at equivalent irradiances, indicating the existence of energy-dissipating cycles that lessened energy transfer from photosystem II to photosystem I. The effective quantum yield of photosystem I decreased only slightly during the daytime and recovered fully in the afternoon, showing that photosystem I was also well protected from photodamage. These results were complemented by analyses of short-term fluorescence induction OKJIP-transients of Kautsky curves, showing 1) that the photosystem II electron donor side was kept fully active throughout the day, 2) that there was no change in the activity of the photosystem II acceptor side, 3) highly efficient electron transport through photosystem I, and 4) an enhanced cyclic electron flow around photosystem I with increasing irradiances. Such non-destructive photoprotective capabilities may in part explain the successful adaptation of the genus *Ulva* to a wide range of irradiance conditions locally as well as globally.

1. Introduction

In addition to changing solar elevation and cloudiness, in- and outgoing tides expose the intertidal zone to highly variable changes in irradiance diurnally. Consequently, the macroalgae growing there may have to perform suitable real-time adjustments in their photosynthetic mechanisms so as to avoid excessive photoinhibition, leading to possible photodamage, during periods of high levels of photosynthetically active radiation (PAR) [1–3] and UV radiation [4,5]. Among those algae, *Ulva* is a globally ubiquitous genus, with an apparently successful adaptation to various and varying environments [6,7], making it a prime candidate for studying adaptational mechanisms on the cellular level.

In the light reactions of photosynthesis, photon energy is converted to stored chemical energy in two steps: Photosystem II (PSII) oxidizes water to form electrons and O_2, and functions in series with photosystem I (PSI) to generate ATP and NADPH, the latter of which are used for reducing CO_2 in the Calvin cycle. Photoinhibition occurs when the harvested light energy exceeds the capacity of electron transport towards the Calvin cycle and/or other energy-dissipating mechanisms [8–10]. Due to the high turnover rate of D1 protein, PSII is often considered sensitive to photoinhibition, being characterized by a decrease of photosynthetic efficiency and an increase of non-photochemical quenching (NPQ). Such dynamic photoinhibition can be repaired within a short time period under dim light or darkness. However, once the balance between damage and repair rate of D1 protein is broken, an irreversible decrease of photosynthetic efficiency would occur due to a chronic photoinhibition (photodamage) [11,12]. Turnover rates of PSI

Abbreviations: CET, cyclic electron transport around PSI; NPQ, non-chemical quenching; OEC, oxygen–evolving complex; PAM, pulse-amplitude modulated; PAR, photosynthetically active radiation; PC, plastocyanin; PQ, plastoquinone; PSI, II, photosystem I, II; P700, PSI reaction center; Q_A, primary electron transport quinone acceptor; qE, energy-dependent quenching; qT, state-transitional quenching; qI, photoinhibitory quenching; qZ, zeaxanthin-cycle dependent quenching; ROS, reactive oxygen species; RC, reaction center

* Corresponding author at: State Key Laboratory of Marine Environmental Science, College of Ocean and Earth Sciences, Xiamen University, Xiamen 361102, China.
E-mail address: ksgao@xmu.edu.cn (K. Gao).

https://doi.org/10.1016/j.algal.2020.102094
Received 3 May 2020; Received in revised form 18 September 2020; Accepted 19 September 2020

subunits are not as high as that of the D1 protein, and anomalies occur under excessive electron flow from PSII [13]. Therefore, any inhibition of PSII activity is thought to protect PSI from photoinhibition or photodamage [13]. In addition, other energy-dissipating mechanisms, i.e. enhanced cyclic electron transport (CET) around PSI, can also protect this photosystem [14,15]. In another aspect, the accumulation of reduced plastoquinone (PQ^{2-}) induced by possible PSI photoinhibition could aggravate the photodamage to PSII [13,16]. From the above, it follows that the interaction of both photosystems should be taken into account when detailing a plant's photosynthetic performance during daily changing irradiances. Once photoinhibition occurs, the concurrent presence of excess excitation energy as well as O_2 can also produce reactive oxygen species (ROS) through the energy transfer from chlorophyll triplet states to O_2 [9,17,18], resulting in photo-oxidative damage to both D1 and iron-sulfur clusters, ultimately leading to photoinhibition of PSII and PSI [13,19,20], as well as of many other cellular functions of any photosynthesizer. Strong interconnectivity might exist between both photosystems, as suggested for higher plants, enabling efficient photosynthetic regulation in response to variable environmental conditions [21]. However, in macroalge, most previous studies [22–27] have merely focused on the PSII performance, and less is known on PSI.

To cope with diurnal fluctuating light environments and reduce the potential damage of accumulated excess energy for photosynthesis, photosynthetic organisms have evolved several acclimative mechanisms, of which the fast recovery during the day should be a prerequisite for the light-adaptation mechanism protecting intertidal algae in their natural environments. Some macroalgae, including the brown (*Padina pavonica*, [22] and *Cystoseira tamariscifolia* [26]), the red (*Ceramium nodulosum*, [24] and *Kappaphycus alvarezii*, [25]) and the green algae (*Ulva rotundata*, [27] and *U. prolifera*, [28]), exhibited a dynamic photoinhibition along with diurnal fluctuations of sunlight, with a midday depression in photosynthesis followed by an afternoon recovery, and different species required different time spans for their photosynthetic machinery to recover under dim or dark conditions. The fastest, and most easily measurable, mechanism for this is NPQ [29,30] (including energy-dependent (qE), state-transitional (qT), photoinhibitory (qI), and zeaxanthin-cycle dependent (qZ) quenching [31–34]), and can be viewed as a photoprotective strategy by dissipating excess energy in the light-harvesting complexes. In addition, an increased efficiency of active PSII reaction centers (RC) [35–37], enhancement of the electron transport capacity at the electron-acceptor side of PSII [38,39], activation of PSI, and CET around PSI [40–43], altering synergies between PSII and PSI [21,44], as well as electron valves to dissipate excess electrons to O_2 [45,46], have also been reported to play a role in regulating the distribution of excitation energy between the two phososystems, thus enabling plants to tolerate stress and maintain optimal rates of photosynthesis. Given that environments in intertidal zones are highly variable, we anticipated that macroalgae thriving there must have evolved acclimative photochemical mechanisms between PSII and PSI to cope with their rapidly changing environments. In macroalgae, the photoprotective function of NPQ have been widely studied, while information about the regulation of photosynthetic electron transport is still lacking and remains to be elucidated.

As a ubiquitous macroalgal genus, photosynthetic traits of *Ulva* spp. have arguably been studied more than those of any other macroalga [2,6,47–49]. In the present study, the diurnal changes in the photosynthetic traits of *U. lactuca* as a result of varying irradiances was measured using a chlorophyll fluorescence technique aimed at characterizing the diurnal variability of photosynthetic activity of both PSII and PSI, and evaluate the regulatory strategies of photosynthetic electron transport.

2. Material and methods

2.1. Experimental set-up

Thalli of *Ulva lactuca*, together with the stones to which they were attached, were collected from the lower intertidal zone of Wuyuan Bay, Xiamen, China (24°31′48″N, 118°10′47″E), and transported to a nearby (within 50 m) outdoor mesocosm facility. There, they were placed in an open water tank, containing flow-through natural seawater from the sampling site (24–26 °C, 32 PSU), at the same depth from which they were collected (~10 cm), and exposed to natural sunlight during 3 clear and sunny days (21st April, 10th and 12th May 2018) of measurements (starting the morning after collection). The below parameters of the light reactions were measured at different times during the day; each individual thallus was independently used and discarded after each measurement, and 5 measurements were carried out at each instance over the 3 days (15 replicates for each measurement). An ANOVA analysis indicated that there was no significant effect of a specific day on any of the measured photosynthetic parameters. The incident solar photosynthetically active radiation (PAR, 400–700 nm) was continuously monitored using a broadband solar radiometer (ELDONET, Real Time Computer Inc., Germany), which is located 16 km away from the experimental site; < 8% of the surface irradiance was attenuated by the ~10 cm water depth (as measured with a diving PAR sensor-equipped in In-situ FIRe (Satlantic, Halifax, NS Canada).

2.2. Measurements of chlorophyll fluorescence and P700 redox states

A dual-wavelength pulse-amplitude modulated (PAM) fluorescence monitoring system (Dual-PAM-100, Walz, Effeltrich, Germany) was employed to simultaneously measure the performance of photosystem II (PSII) and photosystem I (PSI) as well as $P700^+$ absorbance. These measurements were conducted largely as described by Klughammer and Schreiber [50,51] except that the 0.8 s saturating light flash was set to the higher irradiance of ~10,000 μmol photons m^{-2} s^{-1}. The minimal fluorescence (F_0) at pre-dawn, and then during the day following 20 min of dark-adaptation (time of the dark-adaptation was determinted from the pre-experiment, where F_0 showed slightly higher values after 15 than after 20, 30, or 40 mins dark adaption), was measured at the weak irradiance of a modulated red measuring light, and F_m, the maximum fluorescence, was obtained at the end of the saturating-light flash. The stable fluorescence during steady state photosynthesis (F) under light (similar to the incident light levels), and the corresponding maximum steady fluorescence during the saturating-light flash (F_m'), were monitored in 2-h intervals under the diurnally changing solar irradiances. The absorption at 830 and 875 nm measured by the dual-wavelength unit of the instrument was used to evaluate the redox state of P700 [50]. P_m, the maximum $P700^+$ absorption signal, was determined after a saturation flash following a 10-s exposure to far-red light (~300 μmol photons m^{-2} s^{-1}, generated by the instrument). The amplitude of P_m depends on the maximum amount of photo-oxidizable P700, which relates to the quantity of effectively operational PSI complexes. Definitions of P (absorption signal of $P700^+$) and P_m' (the maximum absorption at steady state photosynthesis) are similar to the fluorescence parameters F and F_m', but with a background far-red irradiance (instead of PAR).

To demonstrate the efficiency of photosynthetic electron transport, prompt fluorescence induction kinetics, so-called Kautsky curves, were analyzed using the automated program provided by the Dual-PAM. Samples were dark-adapted for 20 min before the OKJIP-transients were recorded during 300 ms of illumination with saturating (~5000 μmol photons m^{-2} s^{-1}) red light (635 nm).

2.3. Chlorophyll fluorescence and P700 analyses

Chlorophyll fluorescence and P700 redox state measurements were

used to calculate: 1) the effective photochemical quantum yield of PSII, YII [$=(F_m'-F)/F_m'$], also termed $\Delta F/F_m'$, where ΔF equals $F_m'-F$; 2) non-photochemical (NPQ) quenching coefficients of PSII as NPQ [$=(F_m-F_m')/F_m'$]; 3) the effective photochemical quantum yield of PSI, YI [$=(P_m'-P)/P_m$]; and 4) the non-photochemical PSI quantum yield of acceptor-side limited heat dissipation (YNA) and donor-side limited heat dissipation (YND) as YNA $=(P_m-P_m')/P_m$ and YND $=P/P_m$ [51]. The linear slope of re-reduction of $P700^+$, following its oxidation as generated with a modulated measuring light at 830 and 875 nm by turning off the far-red light, was used to evaluate the cyclic electron transport (CET) around PSI. Although the magnitude of the initial slope was small, analysis of the re-reduction kinetics of $P700^+$ has been demonstrated to be relatively straightforward and reliable [52,53].

The efficiency of electron transport between the PSII donor and the PSI acceptor sites was analyzed with the JIP-test [54]. The following parameters were directly obtained from the OKJIP-transients of the Kautsky curves: the minimum fluorescence intensity at the O-step (F_o); the maximum fluorescence intensity at the P-step (F_m); the fluorescence intensity at the 0.3 ms K-step (F_k),; the 3 ms J-step (F_J); and the 30 ms I-step (F_I), following the onset of light. The normalized variable fluorescence at the K-step relative to the amplitude of F_J-F_o (W_k) was calculated as $W_k=(F_k-F_o)/(F_J-F_o)$, the maximum photochemical efficiency of PSII (F_v/F_m) was calculated as $F_v/F_m=(F_m-F_o)/F_m$, the density of PSII reaction centers (RC) per excited cross sections (CS_o) (RC/CS_o) was calculated as $RC/CS_o=F_v/F_m \times V_J/V_K/4 \times F_o$, the probability that a trapped excition moves an electron into the electron transport chain beyond Q_A^- (ψ_{ET2O}) was calculated as $\psi_{ET2O}=1-V_J$, the quantum yield of electron transport (φ_{Eo}) was calculated as $\varphi_{Eo}=(1-F_o/F_m) \times (1-V_J)$, the probability that an electron moves from reduced Q_A beyond PSI (ψ_{RE1O}) was calculated as $\psi_{RE1O}=1-V_I$, and the quantum yield for reduction of the end electron acceptors on the PSI acceptor side (φ_{Ro}) were calculated as $\varphi_{Ro}=(1-F_o/F_m) \times (1-V_I)$. The specific energy fluxes by active RCs were calculated as: absorbed flux [$ABS/RC=4 \times (F_k-F_o) \times F_m/(F_J-F_o) \times F_v$], the trapping flux [$TR_o/RC=4 \times (F_k-F_o)/(F_I-F_o)$], the electron transport flux [$ET_o/RC=4 \times (F_k-F_o) \times (F_m-F_J)/(F_J-F_o) \times F_v$] and the dissipated energy flux ($DI_o/RC=ABS/RC-TR_o/RC$) [37,54,55]. All measured and calculated parameters are presented in Table 1.

2.4. Statistical analyses

Statistical analyses were performed using SPSS 19.0 (SPSS Inc., Chicago, IL, USA). The homogeneity of variance was examined using Levene's test before all statistical analyses. One-way ANOVA and Tukey's test were used to establish differences among treatments. The relationships between measured parameters and irradiance were evaluated using Bayesian inference (B-spline non-linear fitting) with Origin 8.1 (OriginLab, Northampton, MA). Differences were considered to be statistically significant at $p < 0.05$.

3. Results

3.1. Diurnal variations in photochemical and non-photochemical activities of photosystem II and photosystem I

Diurnal fluctuations in photosynthetic active radiation (PAR) of solar irradiance during daytime are shown in Supplementary Fig. 1, reaching highest values of ~1800 μmol photons m^{-2} s^{-1} around 10:00. The effective quantum yields of photosystem II (PSII) and photosystem I (PSI) (YII and YI, respectively) both showed a significant decrease with rising levels of sunlight, and a subsequent increase as the irradiance decreased towards the evening (Fig. 1A). However, there was no significant difference in either YII or YI at similar irradiances during pre-noon and afternoon hours. Simultaneously with the decrease in YII, there was an increase in non-photochemical quenching (NPQ) (Fig. 1B). Unlike YII, NPQ did show significantly higher values during afternoon hours at PAR irradiances similar to those at pre-noon. Corresponding non-photochemical quenching values for the donor and acceptor sides of PSI (YND and YNA, respectively) also showed significant increases with increasing irradiances, but only YNA showed significant differences at similar PAR irradiances during pre-noon and afternoon hours (Fig. 1C, D).

3.2. Diurnal fluctuations in electron transport along photosystem II and photosystem I

The OKJIP patterns of rapid fluorescence induction kinetics, i.e. Kautsky curves, changed diurnally (see Fig. 2A). The amplitude of the fluorescence intensity decreased with the increasing irradiance at noontime and increased in the afternoon. Based on the results from JIP-

Table 1
Measured and calculated parameters used in this paper. Acronyms used: PSII, photosystem II; PSI, photosystem I; RC, reaction center; CS, cross section.

Parameters	Physiological interpretation
Induction curves of PSII and PSI	
F_o, F_m, F, F_m'	Minimal, maximum, stable, and maximum steady fluorescence
P, P_m, P_m'	Real-time, maximum, and maximum steady, absorption signal of $P700^+$
$YII=(F_m'-F)/F_m'$	Effective photochemical quantum yield of PSII
$NPQ=(F_m-F_m')/F_m'$	Non-photochemical quenching of PSII
$YI=(P_m'-P)/P_m$	Effective photochemical quantum yield of PSI
$YNA=(P_m-P_m')/P_m$	Non-photochemical PSI quantum yield of acceptor-side limited heat dissipation
$YND=P/P_m$	Non-photochemical PSI quantum yield of donor-side limited heat dissipation
Kautsky curves	
F_o, F_k, F_J, F_I, F_P	Fluorescence intensity at O, K, J, I, P phases
V_t	Relative variable fluorescence at time t
$W_k=(F_k-F_o)/(F_J-F_o)$	Normalized variable fluorescence at the K-step relative to the amplitude of F_J-F_o
$F_v/F_m=(F_m-F_o)/F_m$	Maximum photochemical efficiency of PSII
$RC/CS_o=F_v/F_m \times V_J/V_K/4 \times F_o$	Density of PSII RC per excited cross sections
$\psi_{ET2O}=1-V_J$	Probability that a trapped excition moves an electron into the electron transport chain beyond Q_A^-
$\varphi_{Eo}=(1-F_o/F_m) \times (1-V_J)$	Quantum yield of electron transport
$\psi_{RE1O}=1-V_I$	Probability that an electron moves from reduced Q_A beyond PSI
$\varphi_{Ro}=(1-F_o/F_m) \times (1-V_I)$	quantum yield for reduction of the end electron acceptors on the PSI acceptor side
$ABS/RC=4 \times (F_k-F_o) \times F_m/(F_J-F_o) \times F_v$	Absorbed flux by active RCs
$TR_o/RC=4 \times (F_k-F_o)/(F_I-F_o)$	Trapping flux by active RCs
$ET_o/RC=4 \times (F_k-F_o) \times (F_m-F_J)/(F_J-F_o) \times F_v$	Electron transport flux by active RCs
$DI_o/RC=ABS/RC-TR_o/RC$	Dissipated energy flux by active RCs

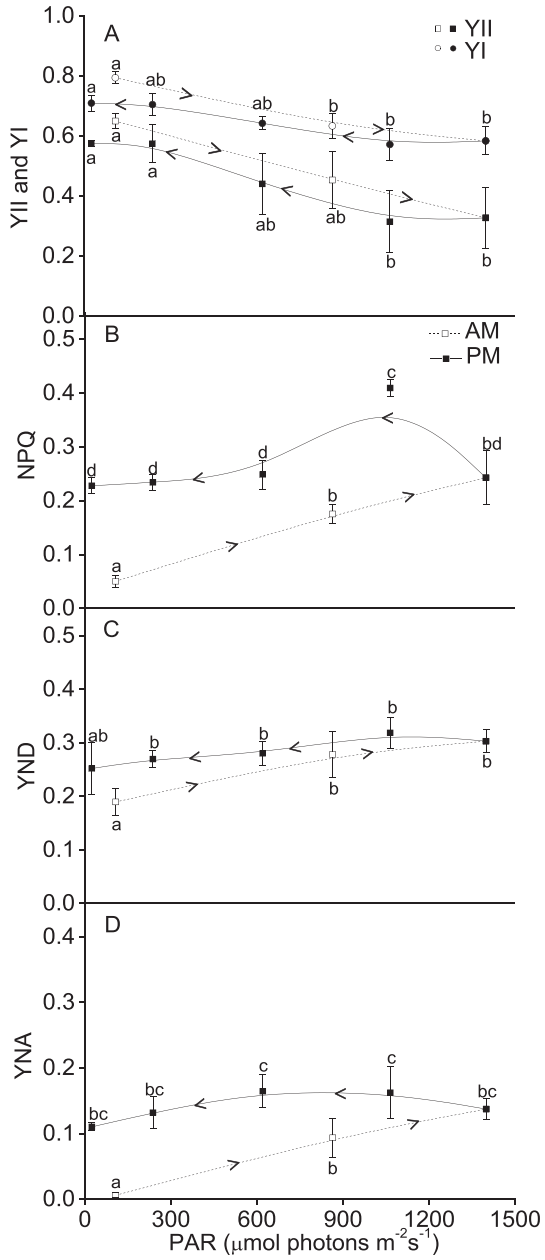

Fig. 1. Effective quantum yields of PSII (YII) and PSI (YI) (panel A), NPQ of PSII (panel B) and NPQs of the donor side (YND, panel C) and of the acceptor side (YNA, panel D) of PSI in *Ulva lactuca* under changing irradiances during morning (6:00–10:00, open symbols and dotted line) and noon/afternoon (10:00–18:00, filled symbols and line); the arrows indicate the progression of morning (right arrow) and afternoon (left arrow) hours. Data represent means ± SD (n = 15; 15 different individuals measured over 3 days, 5 each day). Different letter signify differences along the different diurnal irradiances accoding to Tukey's test. Acronyms used: NPQ, non-photochemical quenching; PSII, photosystem II; PSI, photosystem I; SD, standard deviation.

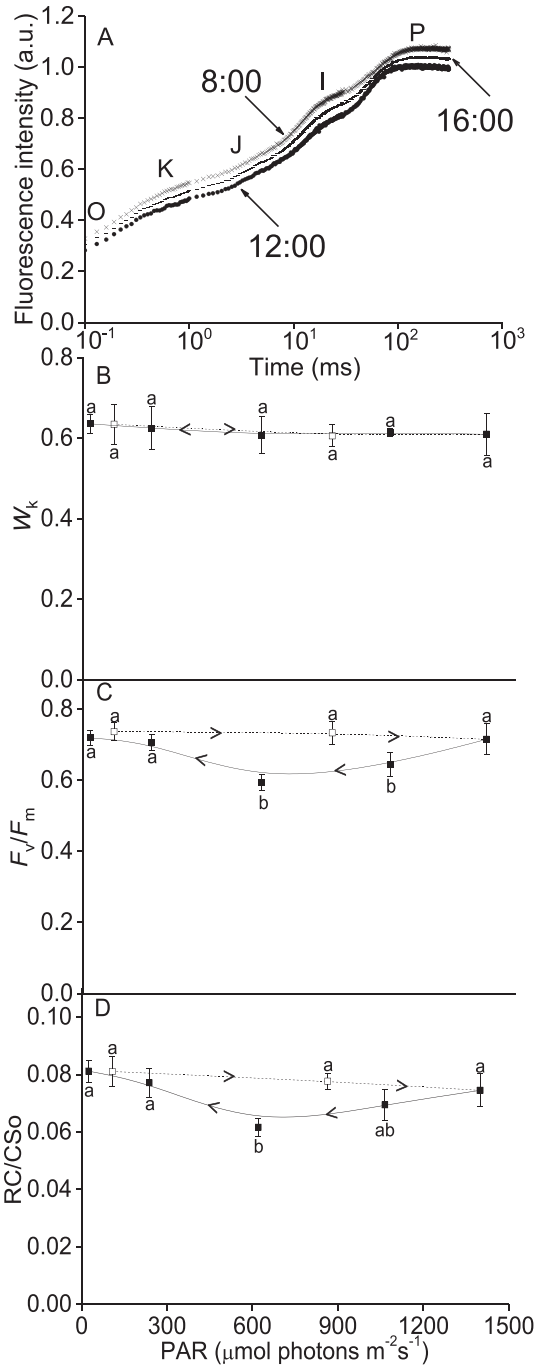

Fig. 2. The short-term rise in prompt fluorescence (Kautsky curves) at 3 different times of the 3-day experimentation (770, 1843 and 655 μmol photons $m^{-2} s^{-1}$) as shown along a logarithmic time scale, SD at each point was < 10% (panel A, see text for the different phases of the curves). The variable fluorescence at the K-phase (W_k, panel B), the maximum quantum yield of PSII (F_v/F_m, C), and the density per excited cross section of PSII RCs (RC/CSo, panel D), were all calculated from the Kautsky curves (n = 15; 15 different individuals measured over 3 days, 5 each day). The arrows indicate the progression of morning (right arrow) and afternoon (left arrows). Data represent the mean ± SD (n = 15; 15 different individuals measured over 3 days, 5 each day). Different letter signify differences along the different diurnal irradiances accoding to Tukey's test. Acronyms used: PSII, photosystem II; RCs, reaction centers; SD, standard deviation.

testing, W_k (the relative variable fluorescence at the K-step per F_J-F_O) did not change significantly throughout the day (Fig. 2B). Daily changes in F_v/F_m as derived from the Kautsky curves showed a trough at 14:00 and recovered completely in the evening (Fig. 2C). Similarly, RC/CS_O [the density of PSII reaction centers (RC) per their excited cross section] exhibited a pattern comparable to that of F_v/F_m (Fig. 2D). Daily changes in ψ_{ET20} and φ_{E0} (the probability that trapped excitons move electrons into the electron transport chain beyond Q_A^-, Fig. 3A, and the quantum yield of electron transport, Fig. 3B, respectively), both calculated from the J-phase, as well as ψ_{RE20} and φ_{R0} (the relative variable fluorescence, Fig. 3C, and the quantum yield of the reduction end of the PSI electron acceptor side, Fig. 3D, respectively), calculated from the I-phase of the Kautsky curves, showed no significant daily fluctuations.

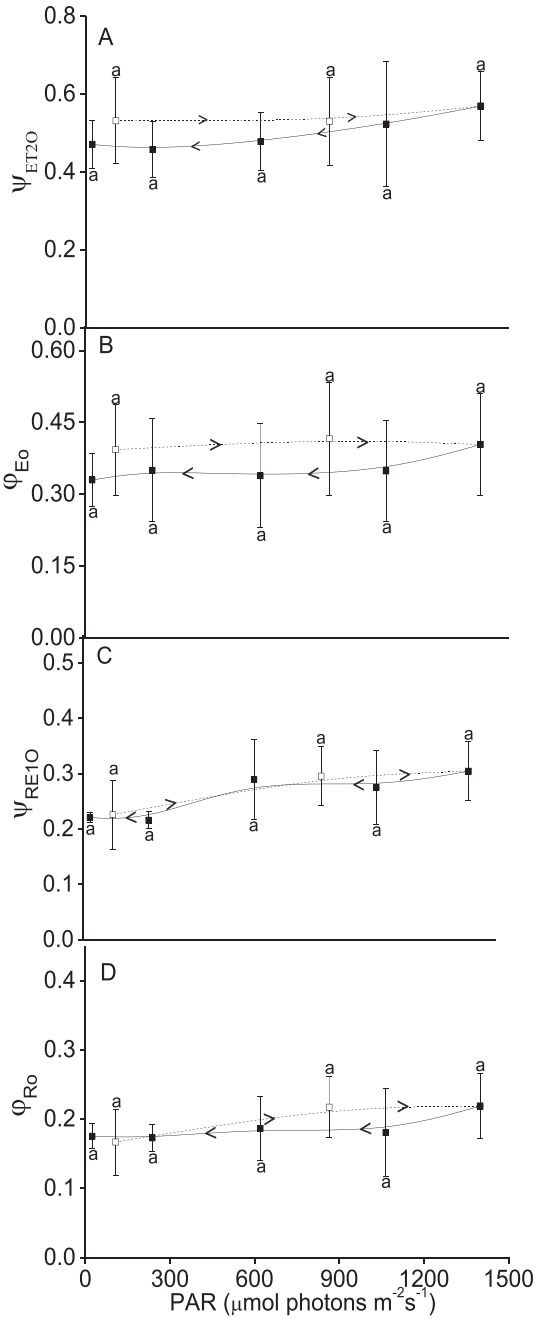

Fig. 3. The probability that trapped excitons move electrons into the electron transport chain beyond Q_A^- (ψ_{ET2O}, panel A) and the quantum yield of electron transport in PSII (φ_{Eo}), both calculated from the J-phase, and the probability that an electron moves from reduced Q_A beyond PSI (ψ_{RE1O}, panel C) and the quantum yield of the reduction end of the PSI electron acceptor side (φ_{Ro}, panel D), both calculated from the I-phase, of the Kautsky curve. The arrows indicate the progression of morning (right arrow) and afternoon (left arrows). Data represent the mean ± SD (n = 15; 15 different individuals measured over 3 days, 5 each day). Different letter signify differences along the different diurnal irradiances accoding to Tukey's test. Acronyms used: Q_A, the primary electron transport acceptor; SD, standard deviation.

3.3. Changes in specific energy fluxes through photosystem II

Daily variations in the absorbed energy flux (ABS/RC, Fig. 4A) and the dissipated energy flux (DIo/RC, Fig. 4D) by active RCs exhibited similar patterns, increasing towards noon and decreasing in the afternoon. However, similarly to NPQ, afternoon values of DIo/RC were significantly higher than those during pre-noon at similar irradiances.

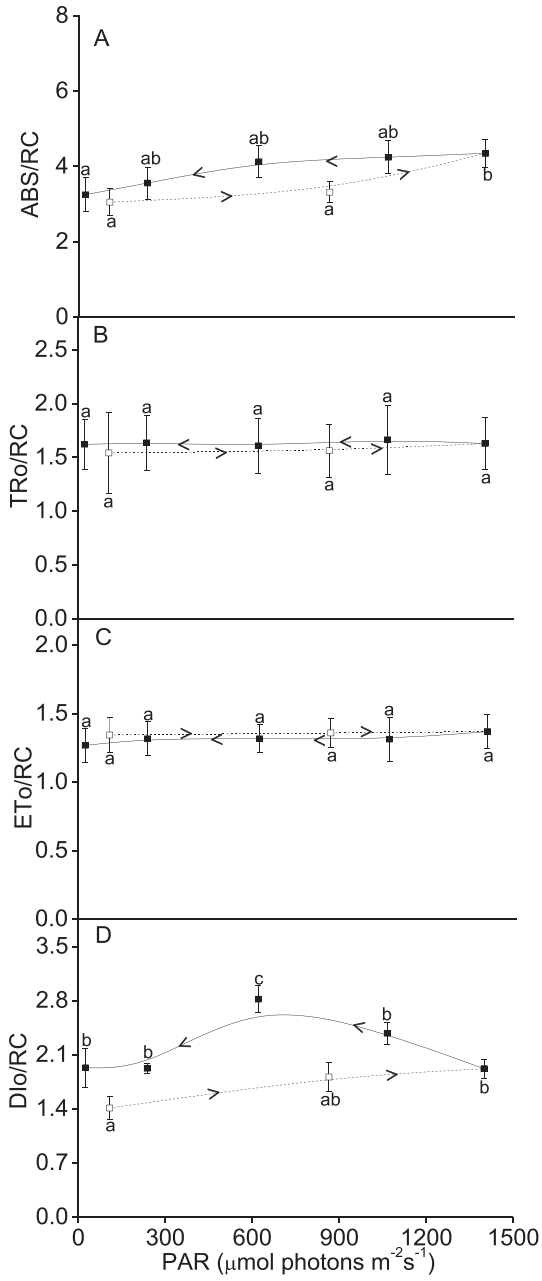

Fig. 4. The absorbed (ABS/RC, panel A), the trapping (TRo/RC, panel B), the electron transport (ETo/RC, panel C) and the dissipated energy (DIo/RC, panel D) fluxes by active reaction centers of PSII, all calculated from the Kautsky curves. The arrows indicate the progression of morning (right arrow) and afternoon (left arrows). Data represent the mean ± SD (n = 15; 15 different individuals measured over 3 days, 5 each day). Different letter signify differences along the different diurnal irradiances accoding to Tukey's test. Acronyms used: RC, reaction center; SD, standard deviation.

No significant diurnal changes were observed in the trapping flux (TRo/RC, Fig. 4B) and the electron transport flux (ETo/RC, Fig. 4C).

3.4. Changes of cyclic electron transport around photosystem I

The $P700^+$ re-reduction measured with the Dual-PAM fluorometer was used to evaluate the cyclic electron transport (CET) around PSI, which increased gradually with increasing irradiances and peaked at 12:00 (Fig. 5). For this parameter, there was a large significant difference at similar irradiances during pre-noon and afternoon.

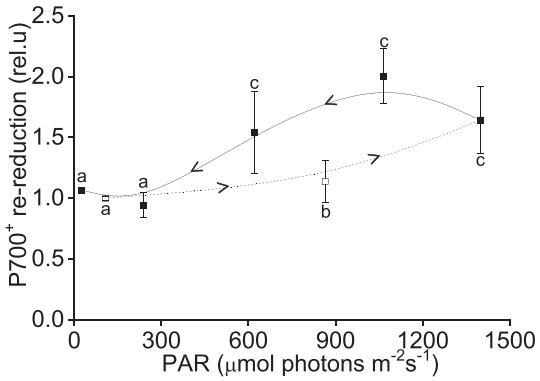

Fig. 5. P700 re-reduction at the various irradiances during morning (6:00–10:00, dotted symbols and line) and noon/afternoon (10:00–18:00, full symbols and line). The arrows indicate the progression of morning (right arrow) and afternoon (left arrows). Data represent the mean ± SD (n = 15; 15 different individuals measured over 3 days, 5 each day). Different letter signify differences along the different diurnal irradiances accoding to Tukey's test. Acronyms used: SD, standard deviation.

4. Discussion

High-light induced photoinhibition reflects a photosynthetic imbalance between the harvested light energy and electron flow through both photosystem II (PSII) and photosystem I (PSI). We found that the maximum (F_v/F_m, Fig. 2C) and the effective (YII, Fig. 1A) quantum yields of PSII in *Ulva lactuca* showed a decline with pre-noon increasing irradiances, and recovered gradually in the afternoon, suggesting the presence of a dynamic type of PSII-related photoinhibition. Changes in F_v/F_m were previously used to estimate macroalgal productivity [24]. In the brown alga *Sargassum thunbergii*, both the photochemical quantuam yield [3] and the photosynthetic rate [56] exhibited a typical diurnal variation, with a midday depression and recovery in the afternoon. Consequently, the photosynthetic performance of *U. lactuca* was here expected to exhibit similar diurnal changes. The fact that YII showed the same values during pre-noon and late afternoon at similar irradiances implied the likelihood that little, if any, photodamage occurred during the day. Rather, this type of dynamic photoinhibition and recovery reflects a sign of energy-dissipating mechanisms being highly efficient in protecting PSII from photodamage. This is contrary to what was found in other marine photosynthesizers, e.g. zooxanthellae-inhabiting corals [57], a red alga (*Chondrus crispus*) [58] as well as a green alga (*U. prolifera*) [28], where PSII needed up to a night of darkness to reinstate morning values. For *U. lactuca*, it shows that its photosynthetic light reactions have evolved better protection mechanisms against high irradiances during the day.

In contrast to PSII, the degradation and subsequent recovery of PSI subunits have generally been reported as slow, and PSI is thus viewed as a more stable photosystem [8,13]. Despite this, previous studies have shown photoinhibition also of PSI, partly related to excessive electron flow from PSII [59–61]. In the present study, the effective quantum yield of PSI (YI) in *U. lactuca* changed in accord with F_v/F_m, but with a slightly decreased amplitude and a faster recovery (Fig. 1A), suggesting the operation of efficient protection mechanisms also for this photosystem. The diurnally sustained efficient activity of PSI could thus act as an electron sink, alleviating the electron back-pressure on PSII by cyclic electron transport (CET, see below), further preventing photodamage also to PSII. Conversely, the fast recovery of YI observed here may also partly relate to the limiting electron transport from PSII to PSI via the down-regulation of PSII activity.

Thermal energy dissipation, i.e. non-photochemical quenching (NPQ), has been viewed as the first line of biochemical defense against photodamage [31]. In the present study, the increasing NPQ with increasing irradiance towards noon, suggests a light-activated photoprotection around PSII. Similarly, the increase of the non-photochemical PSI quantum yield of acceptor-side limited heat dissipation (YNA) and donor-side limited heat dissipation (YND) indicates an up-regulation of energy dissipation at both sides of PSI. Along with the decrease of irradiance in the afternoon, both NPQ, YND and YNA decreased. Such a typical response was also observed in the brown macroalga *Padina pavonica* [22] and the green macroalga *Ulva prolifera* [28], which exhibited a light-dependent adjustment of heat-dissipation of PSII. However, during the afternoon, both NPQ and YNA exhibited higher values in *U. lactuca* at light levels equal with that of morning (Fig. 1B, D), which differ from the rapid and full recovery of NPQ during afternoon observed in the seagrass *Zostera marina* [62]. As previous reported, the sustained NPQ may relate to the accumulation of zeaxanthin; in the brown macroalga *Macrocystis pyrifera* [63,64], the pre-induced xanthophyll cycle resulted in an accumulation of zeaxanthin, which supposedly dissipated light excess energy and alleviated photoinhibition and/or photodamage triggered by the high-light exposure. In *Bryopsis corticulans*, an intertidal green macroalga, the sustained NPQ, unrelated to violaxanthin de-epoxidation, was particularly effective in limiting the impairment/loss of PSII function [30]. Such slowly-relaxed NPQ components are often referred to as photoinhibitory (qI), which could still protect PSII against photodamage [18,32,65]. As *U. lactuca* inhabits the same niche as *B. corticulans*, we speculate that it possesses a similar peculiar molecular mechanism of NPQ, which sustained high values in the afternoon and decreased PSII function, thus endowing *U. lactuca* with a high photoprotective capacity for physiological acclimatization in response to varying environmental irradiance conditions.

A number of studies have reported that cyclic electron transport (CET) around PSI acts works as an important photoprotective mechanism that protect both PSII and PSI [66,67] by 1) generating a higher ΔpH across thylakoid membranes, which is necessary for the formation of NPQ within the antennae complexes [43]; 2) maintaining the Calvin cycle activity by balancing ATP and NADPH and 3) up-regulating Cup proteins [68]. However, these previous studies focus on higher plants, the role of CET in intertidal macroalgae is still unknown. Limited studies showed that values of $P700^+$ re-reduction rates ranged from ~0.3 in the brown macroalga *Sargassum thunbergii* [69] to ~0.2 in the seagrass *Zostera japonica* [44]. While in the present study, the diurnal light-dependent variation of $P700^+$ re-reduction ranged from ~1 to ~2 (Fig. 5), indicating that *U. lactuca* possessed strong CET. Such an active CET is similar with what was observed in the terrestrial evergreen ivy [21]. It is thus reasonable to assume that CET plays an important role in *U. lactuca*'s protection from high irradiances.

In addition to the photoprotective mechanisms mentioned above, photochemical sustainability reflected in the K-phase of Kautsky curves (W_K, Fig. 2B) implied that the O_2-evolving complex of PSII can tolerate high levels of solar irradiances. Although the density of the active reaction centers (RC) decreased (Fig. 2D), the electron flow through PSII kept active, as evidenced by the inapparent changes of the trapping flux (TRo/RC) and the electron transport flux (ETo/RC) by active RCs (Fig. 4B, C). Moreover, the increases in the absorption flux (ABS/RC, Fig. 4A) and dissipated energy flux per RC (DI_0/RC, Fig. 4D) with rising irradiances suggests a high efficiency of heat dissipation by active RCs. Besides, the reversible inactivation of PSII RCs, as demonstrated by a rapid recovery of the density of PSII RCs per excited cross section (RC/CS_o, Fig. 2D), could act as effective exciton traps, efficiently dissipating excitation energy and thus avoiding the occurrence of photodamage, such as found in some terrestrial plants [55,70]. Such adaptive mechanisms regulate the distribution of excitation energy and protect the photosynthetic electron transport chain from over-reduction, as evidenced by a diurnal stability of the probability that a trapped excition moves an electron into that chain beyond Q_A^- (ψ_{ET2O}, Fig. 3A), the quantum yield of electron transport (φ_{Eo}, Fig. 3B), the probability that an electron moves from reduced Q_A beyond PSI (ψ_{RE1O}, Fig. 3C), and the quantum yield for reduction of the end electron acceptors on the PSI

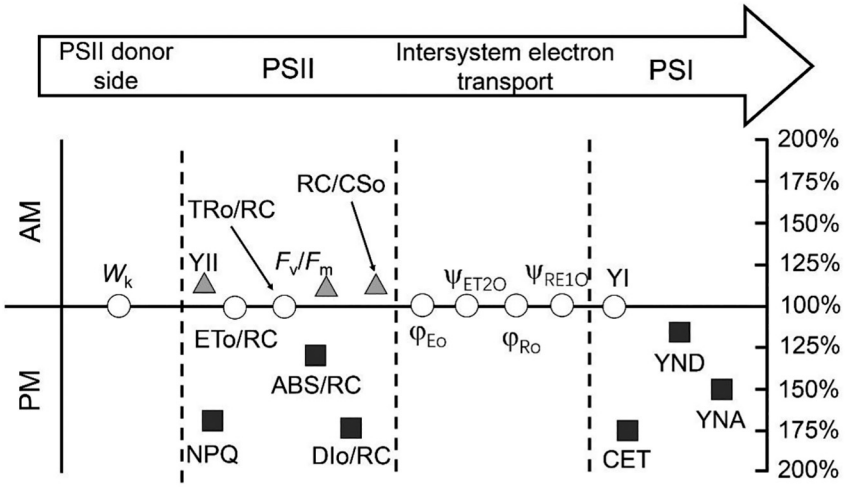

Fig. 6. Integrated diurnal photochemical performances of the green alga *Ulva lactuca*. The arrow directions indicate photosynthetic electron transport. The white circles located in the "100%" line means no significant difference at identical levels of irradiances during pre-noon and afternoon hours; the grey triangles and the black squares mean higher value during A.M. or P.M. periods, respectively.

acceptor side (φ_{Ro}, Fig. 3D).

Integratively, diurnal changes of photosynthetic electron transport showed the following patterns (Fig. 6): 1) the activity of OEC (W_k), PSI (YI), and intersystem electron transport (ψ_{ET2O}, φ_{Eo}, ψ_{RE1O}, φ_{Ro}), the trapping flux (TRo/RC) and the electron transport flux (ETo/RC) per RC, did not change significantly between the morning and afternoon; 2) the activity of PSII (F_v/F_m, YII, and RC/CSo) exhibited higher values in pre-noon hours; and 3) the non-photochemical quenching around both PSII and PSI (NPQ, YND, YNA), the absorption and dissipated energy flux per RC (ABS/RC, DIo/RC), as well as the cyclic electron transport around PSI (CET) exhibited higher values in afternoon. Thus, in conclusion, we provide data to suggest that the photosynthetic light reactions of both PSII and PSI in *U. lactuca* are well-protected from diurnally occurring high irradiances. This is evidenced by a sustained NPQ and efficient CET, as well as other mechanisms leading to efficient harmless dissipation of excess energy. This, in addition to its flexible mode of inorganic carbon utilization [6], may be an important mechanism allowing *Ulva* to grow in altering diurnal irradiances of the intertidal and along depth gradients, as well as globally in various climate zones featuring different irradiance regimes.

Supplementary data to this article can be found online at https://doi.org/10.1016/j.algal.2020.102094.

Fundings

This study was supported by the National Key Research and Development Program (2016YFA0601400), National Natural Science Foundation of China (41720104005, 41721005).

Statement regarding informed consent, human/animal rights

No conflict, informed consent, or animal rights applicable in publishing this article.

CRediT authorship contribution statement

Di Zhang: conceptualization, data collection and curation, data analysis, visualization, writing-original draft, review and editing; Sven Beer: data analysis, formal analysis, writing- review and editing; He Li: data collection, visualization; Kunshan Gao: conceptualization, funding acquisition, project administration, writing- original draft, review and editing.

Declaration of competing interest

The authors declare that they have no known competing financial interests or personal relationships that could have appeared to influence the work reported in this article.

Acknowledgements

The authors are grateful to the laboratory engineers, Xianglan Zeng and Wenyan Zhao, for their technical supports. SB's visit was supported by the State Key Laboratory of Marine Environmental Science (Xiamen University).

References

[1] A. Cabello-Pasini, E. Aguirre-von-Wobeser, F.L. Figueroa, Photoinhibition of photosynthesis in *Macrocystis pyrifera* (Phaeophyceae), *Chondrus crispus* (Rhodophyceae) and *Ulva lactuca* (Chlorophyceae) in outdoor culture systems, J. Photochem. Photobiol. B 57 (2000) 169–178.
[2] B.J. Longstaff, T. Kildea, J.W. Runcie, A. Cheshire, W.C. Dennison, C. Hurd, T. Kana, J.A. Raven, A.W. Larkum, An *in situ* study of photosynthetic oxygen exchange and electron transport rate in the marine macroalga *Ulva lactuca* (Chlorophyta), Photosynth. Res. 74 (2002) 281–293.
[3] Y.Q. Yu, Q.S. Zhang, Y.Z. Tang, X.M. Li, H.L. Liu, L.X. Li, Diurnal changes of photosynthetic quantum yield in the intertidal macroalga *Sargassum thunbergii* under simulated tidal emersion conditions, J. Sea Res. 80 (2013) 50–57.
[4] T. Han, Y.S. Han, J.M. Kain, D.P. Häder, Thallus differentiation of photosynthesis, growth, reproduction, and UV-B sensitivity in the green alga *Ulva pertusa* (Chlorophyceae), J. Phycol. 39 (2003) 712–721.
[5] Y.S. Han, T. Han, UV-B induction of UV-B protection in *Ulva pertusa* (Chlorophyta), J. Phycol. 41 (2005) 523–530.
[6] L. Axelsson, H. Ryberg, S. Beer, Two modes of bicarbonate utilization in the marine green macroalga *Ulva lactuca*, Plant Cell Environ. 18 (1995) 439–445.
[7] M. Björk, L. Axelsson, S. Beer, Why is *Ulva intestinalis* the only macroalga inhabiting isolated rockpools along the Swedish Atlantic coast? Mar. Ecol. Prog. Ser. 284 (2004) 109–116.
[8] S.B. Powles, Photoinhibition of photosynthesis induced by visible light, Annu. Rev. Plant Physiol. 35 (1984) 15–44.
[9] E.M. Aro, I. Virgin, B. Andersson, Photoinhibition of photosystem II. Inactivation, protein damage and turnover, Biochim. Biophys. Acta, B. 1143 (1993) 113–134.
[10] D.P. Häder, M. Lebert, F.L. Figueroa, C. Jiménez, B. Viñegla, E. Perez-Rodriguez, Photoinhibition in Mediterranean macroalgae by solar radiation measured on site by PAM fluorescence, Aquat. Bot. 61 (1998) 225–236.
[11] R. Hill, C.M. Brown, K. DeZeeuw, D.A. Campbell, P.J. Ralph, Increased rate of D1 repair in coral symbionts during bleaching is insufficient to counter accelerated photo-inactivation, Limnol. Oceanogr. 56 (2011) 139–146.
[12] D.A. Campbell, E. Tyystjärvi, Parameterization of photosystem II photoinactivation and repair, Bioch. Biophys. Acta, B. 1817 (2012) 258–265.
[13] K. Sonoike, Photoinhibition of photosystem I, Physiol. Plant. 142 (2011) 56–64.
[14] K. Sonoike, M. Kamo, Y. Hihara, T. Hiyama, I. Enami, The mechanism of the degradation of psaB gene product, one of the photosynthetic reaction center subunits of photosystem I, upon photoinhibition, Photosynth. Res. 53 (1997) 55–63.
[15] M. Tikkanen, N.R. Mekala, E.M. Aro, Photosystem II photoinhibition-repair cycle protects photosystem I from irreversible damage, Bioch. Biophys. Acta, B 2014 (1837) 210–215.
[16] S.E. Tjus, H.V. Scheller, B. Andersson, B.L. Møller, Active oxygen produced during selective excitation of photosystem I is damaging not only to photosystem I, but also to photosystem II, Plant Physiol. 125 (2001) 2007–2015.
[17] E. Tyystjärvi, E.M. Aro, The rate constant of photoinhibition, measured in lincomycin-treated leaves, is directly proportional to light intensity, Proc. Natl. Acad.

Sci. U. S. A. 93 (1996) 2213–2218.
[18] V. Giovagnetti, A.V. Ruban, Discerning the effects of photoinhibition and photoprotection on the rate of oxygen evolution in Arabidopsis leaves, J. Photochem. Photobiol. B 152 (2015) 272–278.
[19] T. Sejima, D. Takagi, H. Fukayama, A. Makino, C. Miyake, Repetitive short-pulse light mainly inactivates photosystem I in sunflower leaves, Plant Cell Physiol. 55 (2014) 1184–1193.
[20] D. Takagi, S. Takumi, M. Hashiguchi, T. Sejima, C. Miyake, Superoxide and singlet oxygen produced within the thylakoid membranes both cause photosystem I photoinhibition, Plant Physiol. 171 (2016) 1626–1634.
[21] D. Zhang, Q.S. Zhang, X.Q. Yang, Z.T. Sheng, G.N. Nan, The alternation between PSII and PSI in ivy (*Hedera nepalensis*) demonstrated by in vivo chlorophyll a fluorescence and modulated 820 nm reflection, Plant Physiol. Biochem. 108 (2016) 499–506.
[22] D.P. Häder, M. Lebert, J. Mercado, J. Aguilera, S. Salles, S. Flores-Moya, C. Jiméz, Figueroa FL photosynthetic oxygen production and PAM fluorescence in the brown alga *Padina pavonica* measured in the field under solar radiation, Mar. Biol. 127 (1996) 61–66.
[23] R.T. Abdala-Díaz, A. Cabello-Pasini, E. Pérez-Rodríguez, R.C. Álvarez, F.L. Figueroa, Daily and seasonal variations of optimum quantum yield and phenolic compounds in *Cystoseira tamariscifolia* (Phaeophyta), Mar. Biol. 148 (3) (2006) 459–465.
[24] G. Magnusson, Diurnal measurements of F_v/F_m used to improve productivity estimates in macroalgae, Mar. Biol. 130 (2) (1997) 203–208.
[25] Ryuta Terada, Triet Duy Vo, Gregory N. Nishihara, Keisaku Shioya, Satoshi Shimada, Shigeo Kawaguchi, The effect of irradiance and temperature on the photosynthesis and growth of a cultivated red alga *Kappaphycus alvarezii* (Solieriaceae) from Vietnam, based on in situ and in vitro measurements, J. Appl. Phycol. 28 (2016) 457–467.
[26] Ryuta Terada, Kazuya Matsumoto, Iris Ann Borlongan, Yuki Watanabe, Gregory N. Nishihara, Hikaru Endo, Satoshi Shimada, The combined effects of PAR and temperature including the chilling-light stress on the photosynthesis of a temperate brown alga, *Sargassum patens* (Fucales), based on field and laboratory measurements, J. Appl. Phycol. 30 (2018) 1893–1904.
[27] W.J. Henley, G. Levavasseur, L.A. Franklin, S.T. Lindley, J. Ramus, C.B. Osmond, Diurnal responses of photosynthesis and fluorescence in *Ulva rotundata* acclimated to sun and shade in outdoor culture, Mar. Ecol. Prog. Ser. (1991) 19–28.
[28] X. Zhao, X. Tang, S. Hu, Y. Zhong, T. Qu, Y. Wang, Photosynthetic response of floating *Ulva prolifera* to diurnal changes of in-situ environments on the sea surface, J. Oceanol. Limnol. 37 (2019) 589–599.
[29] A.V. Ruban, Nonphotochemical chlorophyll fluorescence quenching: mechanism and effectiveness in protecting plants from photodamage, Plant Physiol. 170 (2016) 1903–1916.
[30] V. Giovagnetti, G. Han, M.A. Ware, P. Ungerer, X. Qin, W.D. Wang, T.Y. Kuang, J.R. Shen, A.V. Ruban, A siphonous morphology affects light-harvesting modulation in the intertidal green macroalga *Bryopsis corticulans* (Ulvophyceae), Planta 247 (2018) 1293–1306.
[31] W.W. Adams III, B. Demmig-Adams, Carotenoid composition and down regulation of photosystem II in three conifer species during the winter, Physiol. Plant. 92 (1994) 451–458.
[32] A.V. Ruban, M.P. Johnson, C.D. Duffy, The photoprotective molecular switch in the photosystem II antenna, Biochim. Biophys. Acta, B 2012 (1817) 167–181.
[33] B. Demmig-Adams, S.C. Koh, C.M. Cohu, O. Muller, J.J. Stewart, W.W. Adams, Nonphotochemical fluorescence quenching in contrasting plant species and environments, in: B. Demming-Adams, G. Garab, W.W. Adams, IIIGovindjee (Eds.), Nonphotochemical Quenching and Energy Dissipation in Plants, Algae and Cyanobacteria, Springer, Dordrecht, 2014, pp. 531–552.
[34] R. Goss, B. Lepetit, Biodiversity of NPQ, J. Plant Physiol. 172 (2015) 13–32.
[35] P. Eullaffroy, C. Frankart, A. Aziz, M. Couderchet, C. Blaise, Energy fluxes and driving forces for photosynthesis in *Lemna minor* exposed to herbicides, Aquat. Bot. 90 (2009) 172–178.
[36] M.C. Perron, P. Juneau, Effect of endocrine disrupters on photosystem II energy fluxes of green algae and cyanobacteria, Environ. Res. 111 (2011) 520–529.
[37] A. Stirbet, Govindjee, On the relation between the Kautsky effect (chlorophyll a fluorescence induction) and photosystem II: basics and applications of the OJIP fluorescence transient, J. Photochem. Photobiol. B 104 (2011) 236–257.
[38] T.D. Hall, D.R. Chastain, P.J. Horn, K.D. Chapman, J.S. Choinski Jr., Changes during leaf expansion of ΦPSII temperature optima in *Gossypium hirsutum* are associated with the degree of fatty acid lipid saturation, J. Plant Physiol. 171 (2014) 411–420.
[39] Y. Duan, M. Zhang, J. Gao, P. Li, V. Goltsev, F. Ma, Thermotolerance of apple tree leaves probed by chlorophyll a fluorescence and modulated 820 nm reflection during seasonal shift, J. Photochem. Photobiol. B 152 (2015) 347–356.
[40] N.G. Bukhov, C. Wiese, S. Neimanis, U. Heber, Heat sensitivity of chloroplasts and leaves: leakage of protons from thylakoids and reversible activation of cyclic electron transport, Photosynth. Res. 59 (1999) 81–93.
[41] P. Joliot, A. Joliot, Cyclic electron flow in C3 plants, Biochim. Biophys. Acta, B 1757 (2006) (2006) 362–368.
[42] T.D. Sharkey, R. Zhang, High temperature effects on electron and proton circuits of photosynthesis, J. Integr. Plant Biol. 52 (2010) 712–722.
[43] P. Joliot, G.N. Johnson, Regulation of cyclic and linear electron flow in higher plants, Proc. Natl. Acad. Sci. U. S. A. 108 (2011) 13317–13322.
[44] D. Zhang, Q.S. Zhang, X.Q. Yang, Adaptive strategies of *Zostera japonica* photosynthetic electron transport in response to thermal stress, Mar. Biol. 164 (2017) 35.
[45] F. Chaux, A. Burlacot, M. Mekhalfi, P. Auroy, S. Blangy, P. Richaud, G. Peltier, Flavodiiron proteins promote fast and transient O_2 photoreduction in *Chlamydomonas*, Plant Physiol. 174 (2017) 1825–1836.
[46] G. Shimakawa, A. Murakami, K. Niwa, Y. Matsuda, A. Wada, C. Miyake, Comparative analysis of strategies to prepare electron sinks in aquatic photoautotrophs, Photosynth. Res. 139 (2019) 401–411.
[47] S. Beer, A. Israel, Z. Drechsler, Y. Cohen, Photosynthesis in *Ulva fasciata*: V. Evidence for an inorganic carbon concentrating system, and ribulose-1,5-bisphosphate carboxylase/oxygenase CO_2 kinetics, Plant Physiol. 94 (1990) 1542–1546.
[48] Z. Drechsler, S. Beer, Utilization of inorganic carbon by *Ulva lactuca*, Plant Physiol. 97 (1991) 1439–1444.
[49] J. Xu, K. Gao, Future CO_2-induced ocean acidification mediates the physiological performance of a green tide alga, Plant Physiol. 160 (2012) 1762–1769.
[50] C. Klughammer, U. Schreiber, An improved method, using saturating light pulses, for the determination of photosystem I quantum yield via $P700^+$-absorbance changes at 830 nm, Planta 192 (1994) 261–268.
[51] C. Klughammer, U. Schreiber, Complementary PS II quantum yields calculated from simple fluorescence parameters measured by PAM fluorometry and the saturation pulse method, PAM application notes 1 (2008) 27–35 http://www.walz.com.
[52] D.Y. Fan, Q. Nie, A.B. Hope, W. Hillier, B.J. Pogson, W.S. Chow, Quantification of cyclic electron flow around photosystem I in spinach leaves during photosynthetic induction, Photosynth. Res. 94 (2007) 347–357.
[53] D.Y. Fan, D. Fitzpatrick, R. Oguchi, W. Ma, J. Kou, W.S. Chow, Obstacles in the quantification of the cyclic electron flux around photosystem I in leaves of C3 plants, Photosynth. Res. (2016) 1–13.
[54] B.J. Strasser, R.J. Strasser, Measuring fast fluorescence transients to address environmental questions: the JIP-test, in: P. Mathis (Ed.), Photosynthesis: From Light to Biosphere, Vol V Kluwer Academic Publishers, The Netherlands, 1995, pp. 977–980.
[55] R.J. Strasser, M. Tsimilli-Michael, A. Srivastava, G.C. Papageorgiou, Govindjee, Analysis of the chlorophyll a fluorescence transient, Chlorophyll a Fluorescence, Springer, Dordrecht, 2004, pp. 321–362.
[56] K. Gao, I. Umezaki, Studies on diurnal photosynthetic performance of *Sargassum thunbergii* I. Changes in photosynthesis under natural sunlight, Jpn. J. Phycol. 37 (1989) 89–98.
[57] G. Winters, Y. Loya, R. Röttgers, S. Beer, Photoinhibition in shallow-water colonies of the coral *Stylophora pistillata* as measured in situ, Limnol. Oceanogr. 48 (2003) 1388–1393.
[58] D. Hanelt, K. Huppertz, W. Nultsch, Daily course of photosynthesis and photoinhibition in marine macroalgae investigated in the laboratory and field, Mar. Ecol. Prog. Ser. 97 (1993) 31–37.
[59] K. Sonoike, Selective photoinhibition of photosystem I in isolated thylakoid membranes from cucumber and spinach, Plant Cell Physiol. 36 (1995) 825–830.
[60] K. Sonoike, Photoinhibition of photosystem I: its physiological significance in the chilling sensitivity of plants, Plant Cell Physiol. 37 (1996) 239–247.
[61] Z. Zhang, Y. Jia, H. Gao, L. Zhang, H. Li, Q. Meng, Characterization of PSI recovery after chilling-induced photoinhibition in cucumber (*Cucumis sativus* L.) leaves, Planta 234 (2011) 883–889.
[62] X.Q. Yang, Q.S. Zhang, D. Zhang, Z.T. Sheng, Light intensity dependent photosynthetic electron transport in eelgrass (*Zostera marina* L.), Plant Physiol. Biochem. 113 (2017) 168–176.
[63] E. García-Mendoza, M.F. Colombo-Pallotta, The giant kelp *Macrocystis pyrifera* presents a different nonphotochemical quenching control than higher plants, New Phytol. 173 (2007) 526–536.
[64] E. Garcia-Mendoza, H. Ocampo-Alvarez, Photoprotection in the brown alga *Macrocystis pyrifera*: evolutionary implications, J. Photochem. Photobiol. B 104 (2011) 377–385.
[65] M.A. Ware, E. Belgio, A.V. Ruban, Photoprotective capacity of non-photochemical quenching in plants acclimated to different light intensities, Photosynth. Res. 126 (2015) 261–274.
[66] Y.N. Munekage, B. Genty, G. Peltier, Effect of PGR5 impairment on photosynthesis and growth in *Arabidopsis thaliana*, Plant Cell Physiol. 49 (2008) 1688–1698.
[67] W. Huang, S.J. Yang, S.B. Zhang, J.L. Zhang, K.F. Cao, Cyclic electron flow plays an important role in photoprotection for the resurrection plant *Paraboearufescens* under drought stress, Planta 235 (2012) 819–828.
[68] X. Han, N. Sun, M. Xu, H. Mi, Co-ordination of NDH and Cup proteins in CO_2 uptake in cyanobacterium Synechocystis sp. PCC 6803, J. Exp. Bot. 68 (2017) 3869–3877.
[69] D. Zhang, Q.S. Zhang, X.Q. Yang, Seasonal dynamics of photosynthetic activity in the representive brown macroalgae *Sargassum thunbergii* (Sargassaceae Phaeophyta), Plant Physiol. Biochem. 120 (2017) 88–94.
[70] H.Y. Lee, Y.N. Hong, W.S. Chow, Photoinactivation of photosystem II complexes and photoprotection by non-functional neighbours in *Capsicum annuum* L. leaves, Planta 212 (2001) 332–342.